Macromolecules
ARTICLE

Macromolecules **2010**, *43*, 10253–10261 **10253**
DOI: 10.1021/ma102369q

Effect of Dimensionality in Dendrimeric and Polymeric Fluorescent Materials for Detecting Explosives

Hamish Cavaye, Paul E. Shaw, Xin Wang, Paul L. Burn,* Shih-Chun Lo, and Paul Meredith*

Centre for Organic Photonics & Electronics, The University of Queensland, Brisbane, Queensland 4072, Australia

Received October 18, 2010; Revised Manuscript Received November 15, 2010

ABSTRACT: Steady-state Stern−Volmer analysis is uniformly used to assess in solution the efficiency of a sensing molecule for a particular analyte. We use a combination of steady-state Stern−Volmer analysis and time-resolved photoluminescence (TRPL) to determine the underlying mechanisms by which fluorescent sensing materials comprised of fluorene-based chromophores sense nitro-based explosive analytes. The ability of two first-generation dendrimers comprised of bifluorene-containing chromophores to sense explosive analytes was compared with the chemically related polymer poly(9,9-di-*n*-octylfluoren-2,7-diyl). One dendrimer was planar with a single chromophore with the second having four chromophores tetrahedrally arranged around an adamantyl center. All the materials had high photoluminescence quantum yields of around 90% and were able to sense explosive analytes via quenching of their fluorescence. The three-dimensional dendrimer based upon the adamantyl core was found to have the highest Stern−Volmer constants for all the analytes tested with the planar dendrimer also proving to be on average superior to the polymer. The TRPL measurements showed that sensing occurred by a combination of collisional and static quenching with the proportion of collisional quenching being based on the number of aromatic units in the analyte. Steady-state fluorescence polarization anisotropy measurements of the three materials revealed that for the three-dimensional dendrimer an exciton can migrate between all of the chromophores, meaning that an exciton formed on one chromophore of the dendrimer can be quenched by an analyte interacting with a second chromophore. This gives rise to the potential for sensing response amplification and explains its superior performance to the planar dendrimer and polymer.

Introduction

Whether for use in the military, at airport security, or in the remediation of minefields and munitions factories, the rapid and reliable detection of explosive compounds is becoming increasingly important. There are many different explosive compounds; however, a large number have a similar chemical structure, often including a nitro or nitroaromatic group. Arguably the most well-known explosive compound is 2,4,6-trinitrotoluene (TNT). TNT is a common and inexpensive compound that is found in at least 15 standard explosive compositions[1] and is often the primary energetic material in land mines.[2,3] Another compound of interest is 2,3-dimethyl-2,3-dinitrobutane (DMNB), which is a taggant added to all commercially manufactured plastic explosives to aid in their detection by trained canines.

Many technologies[4] designed to replace dogs are already able to detect trace levels of nitrated explosives. Such technologies include, but are not limited to, ion mobility spectrometry (IMS),[5] colorimetric detectors,[6] electrochemical sensors,[7] and surface acoustic wave (SAW) devices.[8] However, many of these systems are not truly portable or require solid samples or swipes to be collected for analysis. Luminescence quenching-based systems offer some advantages in that they can be miniaturized for truly hand-held devices and are able to detect vapor-phase analyte for standoff detection.

A wide variety of luminescence-based sensors for explosives have been reported including small molecules,[9,10] metal complexes,[11−13] metal−organic frameworks,[14] carbon nanotubes,[15,16] polymers,[17−20] and dendrimers.[21−26] The majority of these sensors rely upon an oxidative quenching mechanism,[20,27] in which the sensing chromophore undergoes charge transfer of the photoexcited electron to the analyte. The oxidation of the excited state quenches the photoluminescence (PL), indicating that the analyte is present. Therefore, the relative energy levels of the sensor excited state and the analyte electron affinity are very important. In addition, for polymer-based sensors it has been reported that the attachment of bulky groups to the chain is necessary to ensure rapid ingress of the analyte into the sensing film.[28] Hence, it is not only the electronic factors that are important in sensing but also how the analyte can physically interact with the sensing material. The leading luminescence-based sensors are currently based on conjugated polymers with hand-held devices already in the market.[29,30]

While many of these luminescent materials have excellent sensitivities to nitroaromatic compounds, improving the selectivity of the sensor molecule and reducing false positives is an ongoing area of interest. A detailed understanding of the fundamental interactions occurring between the fluorescent sensing compound and the analytes would aid in the design of next-generation sensors with improved selectivity. In this paper we study the effect of molecular dimensionality on the sensitivity and selectivity of two fluorescent dendrimers in solution and compare them with a related fluorescent polymer based upon the fluorene moiety (Figure 1). We performed these measurements using dilute solutions with the aim of studying the ability of individual macromolecules to sense and hence compare the effect of including single or multiple chromophores per sensing unit.

Light-emitting dendrimers are a relatively new class of macromolecules that have already been successful in light-emitting

*Corresponding authors. E-mail: p.burn2@uq.edu.au (P.L.B.); meredith@physics.uq.edu.au (P.M.).

Published on Web 12/02/2010

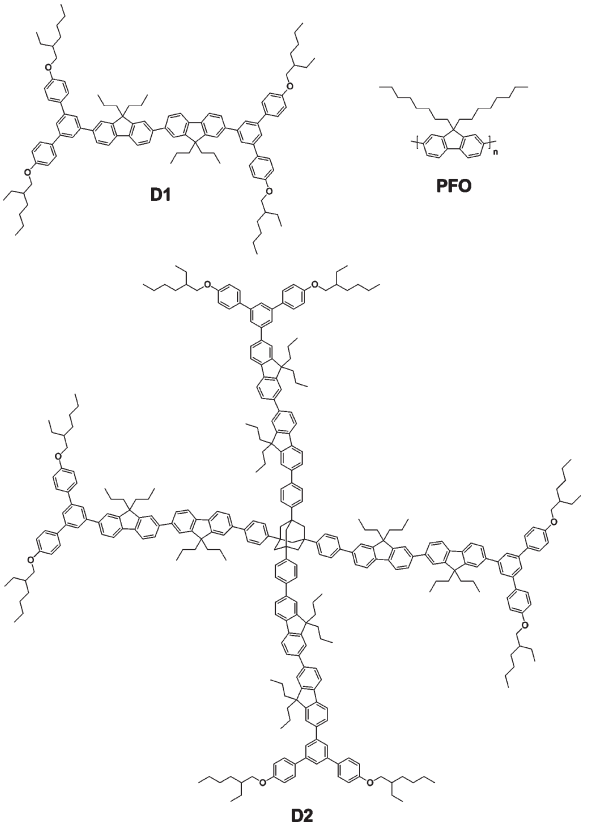

Figure 1. Three sensing compounds used in this study. A first-generation bifluorene-cored dendrimer (D1), poly(9,9-di-*n*-octylfluoren-2,7-diyl) (PFO), and a first-generation adamantyl-cored bifluorene dendrimer (D2).

diodes.[31−34] Dendrimers consist of a core, branching dendrons, and surface groups, the latter being primarily responsible for solubility. A major advantage of dendrimers over other macromolecules, such as polymers, is that they are monodisperse and their modular branched structure allows a high level of control over the properties of the final compound.

The physical and sensing properties of dendrimer D1 (Figure 1) in thin films have been reported previously.[22] D1 is essentially planar with a single 9,9,9′,9′-tetra-*n*-propyl-2,2′-bifluorene containing chromophore, and it was of interest to see what the effect of increasing the number of chromophores and dimensionality was on the sensing ability of dendritic materials. D2 is a higher dimensionality dendrimer (Figure 1) due to the adamantyl center and has four near identical chromophores to that found in D1. Finally, poly(9,9-di-*n*-octylfluoren-2,7-diyl) (PFO) was chosen to allow the comparison of the two dendrimers to a linear polymer comprised of fluorene chromophores.[35]

Experimental Section

Synthesis and Characterization. Solvents were distilled before use. When solvent mixtures are reported, the proportions are given by volume. Dichloromethane (CH_2Cl_2) used for the electrochemical experiments was dried over calcium hydride, distilled, and then stored over activated 4 Å molecular sieves. Tetrahydrofuran (THF) used for anhydrous reactions was stirred over sodium/benzophenone and then distilled immediately prior to use. THF used for electrochemical experiments was then further distilled from lithium aluminium hydride immediately prior to use.

^{1}H and ^{13}C NMR spectra were recorded on a Bruker AV300 or Bruker AV500 spectrometer. Chemical shifts are reported in parts per million (ppm) and are referenced to the residual solvent peak (chloroform, ^{1}H = 7.27 ppm, ^{13}C = 77.0 ppm). Coupling constants (J) are given in hertz (Hz) and are quoted to the nearest 0.5 Hz. Peak multiplicities are described in the following way: doublet (d), doublet of doublets (dd), multiplet (m), broad (br); peak identities are described as EtHeO = 2-ethylhexyloxy H, Pr-H = *n*-propyl H, bp-H = branching phenyl H, sp-H = surface phenyl H, pin-CH_3 = pinacolate H, Ad-H_2 = adamantyl H, and Fl-H = fluorenyl H. Elemental analysis was performed by the Microanalytical Service within the School of Chemistry and Molecular Biosciences, University of Queensland, Australia. Mass spectra were recorded on an Applied Biosystems Voyager MALDI-TOF mass spectrometer in positive reflector mode using either 1,8,9-anthracenetriol (Dith) or (*E*)-2-[3-(4-*tert*-butylphenyl)-2-methyl-2-propenylidene]malononitrile (DCTB) as the matrix compound. Absorption spectra were measured on a Varian Cary 5000 UV−vis−NIR spectrophotometer using spectroscopic grade dichloromethane or tetrahydrofuran as the solvent. Steady-state fluorescence spectra were recorded on a Horiba Jobin-Yvon Fluorolog Tau3 or Horiba Jobin-Yvon Fluoromax 4 spectrometer. Thermal gravimetric analyses were performed with a Perkin-Elmer STA 6000 under nitrogen, and results are reported as the temperature at which a 5% weight loss ($T_{5\%}$) was observed. Differential scanning calorimetry was performed with a Perkin-Elmer Diamond DSC. Compounds **2** and **3** both had glass transition temperatures (T_gs) with a second thermal transition at a slightly higher temperature, which we could not assign.

Cyclic voltammetry oxidation ($E_{1/2(Ox)}$) and reduction ($E_{1/2(Red)}$) potentials were recorded with a BASi EpsilonEC using either a platinum or glassy carbon working electrode, a platinum auxiliary electrode, and a 0.1 M $Ag/AgNO_3$ in acetonitrile reference electrode. Dichloromethane was used as the solvent for oxidations, and tetrahydrofuran was used as the solvent for reductions. The concentration of active species was 1 mM. 0.1 M tetra(*n*-butyl)ammonium perchlorate was used as the electrolyte, and the scan rate was 300 or 500 mV s^{-1}. Peak positions were confirmed with differential pulse voltammetry (20 mV s^{-1}, 4 mV steps, 50 ms pulse width, 200 ms pulse period, 50 mV pulse amplitude). The potentials are reported relative to the ferrocenium/ferrocene couple under identical conditions.[36]

Poly(9,9-di-*n*-octylfluoren-2,7-diyl) (PFO) ($\overline{M}_w$ = 13 000, PDI = 3.4) was purchased from American Dye Source, Inc., and used as received. Solutions of PFO were left to stir overnight before use. All quenching analytes were purchased from Sigma-Aldrich and used without further purification. D1 was prepared following a literature procedure.[22]

Spectroscopy and Quenching. Solution photoluminescence quantum yields (PLQY) were measured using the relative method with quinine sulfate in 0.5 M sulfuric acid as the reference (PLQY = 55%).[37] The excitation wavelength for D1 and D2 was 310 nm, and the excitation wavelength for PFO was 360 nm. The solutions were measured under ambient conditions, and the error in the PLQY is ±5% of the reported value.

For the Stern−Volmer measurements the analytes were dissolved in the dendrimer or polymer solution so that the concentration of dendrimer or polymer was unchanged throughout the experiment and only the analyte concentration varied. For the steady-state measurements 2.5 mL of dendrimer or polymer solution (peak absorbance of ∼0.1) was placed in a 10 mm path length fluorescence cuvette, and both absorbance and emission spectra (excited at the peak absorbance wavelength) were recorded. Sequential additions of a known volume of analyte solution were then added to the cuvette, and the absorption and emission spectra were recorded after each addition. The concentration of analyte was chosen so that the maximum absorbance of the solution at the excitation wavelength did not exceed ∼0.6. This ensured that the data could be reliably corrected for absorbance of the excitation by the analyte as well as the inner filter effect.[21,38]

For the time-resolved fluorescence measurements, dilute solutions of the sensing materials were excited with ~70 fs pulses at wavelengths of ~375 nm (for D1 and D2) or ~390 nm (for PFO) at a repetition rate of 80 MHz using the frequency-doubled output of a Spectra-Physics Tsunami Ti:sapphire laser. The fluorescence decays were measured at 395 nm [400 nm for measurements with duroquinone (DQ)] for D1 and D2 and 414 nm for PFO using a Picoquant TCSPC setup with an instrument response function (IRF) with a FWHM of ~300 ps. All fits to the time-resolved data were performed with convolution of the IRF.

For the fluorescence anisotropy measurements, emission and detection polarizers were incorporated into the Fluorolog Tau3. Dilute solutions of the sensing materials were excited at the peak absorption with vertically polarized excitation and the emission measured with the detection polarizer aligned for vertically (I_{VV}) and then horizontally (I_{VH}) polarized emission. The same fluorescence measurements were then repeated with horizontally polarized excitation (to give I_{HV} and I_{HH}). The anisotropy r was calculated as[39]

$$r = \frac{I_{VV} - GI_{VH}}{I_{VV} + 2GI_{VH}} \quad (1)$$

where G is a gratings correction factor given by

$$G = \frac{I_{HV}}{I_{HH}} \quad (2)$$

Synthesis. *7-Bromo-7′-iodo-9,9,9′,9′-tetra-n-propyl-2,2′-bifluorene* (***1***). 7-Bromo-9,9,9′,9′-tetra-*n*-propyl-2,2′-bifluorene[40] (5.0 g, 8.7 mmol) and *N*-iodosuccinimide (2.1 g, 9.5 mmol) were dissolved in chloroform (100 mL). The reaction vessel was deoxygenated by applying vacuum and then backfilling with argon four times. Trifluoroacetic acid (4 mL) was added before deoxygenating a further three times. The reaction was stirred in the dark and heated at 60 °C for 20 h. Upon cooling to room temperature, the reaction was quenched with aqueous sodium metabisulfite (0.5 M, 100 mL), and the layers were separated. The aqueous phase was extracted with chloroform (20 mL), and the combined organic layers were neutralized with saturated aqueous sodium bicarbonate (2 × 50 mL), washed with water (50 mL) and brine (100 mL), dried over magnesium sulfate, and filtered. The solvent was removed to afford **1** as a tan solid (6.2 g, quantitative). Found: C 64.9, H 5.8 ($C_{38}H_{40}BrI$ requires C 64.9, H 5.7). ^{1}H NMR (500 MHz, $CHCl_3$) δ [ppm]: 7.75 (brdd, 2H, J = 8.0 Hz, J = 1.0 Hz, Fl-H), 7.71 (d, 1H, J = 1.4 Hz, Fl-H), 7.69 (dd, 1H, J = 8.0 and 1.5 Hz, Fl-H), 7.64 (dd, 2H, J = 8.0 and 1.5 Hz, Fl-H), 7.59−7.61 (m, 3H, Fl-H), 7.47−7.52 (m, 3H, Fl-H), 1.96−2.07 (m, 8H, Pr−H), 0.70−0.77 (m, 20 H, Pr−H). ^{13}C NMR (125 MHz, $CHCl_3$) δ [ppm]: 153.4, 153.2, 151.1, 150.9, 140.9, 140.8, 140.4, 139.7, 139.4, 139.3, 135.9, 132.1, 130.0, 126.3(0), 126.2(8), 126.2, 121.4, 121.3(5), 121.2(8), 121.1, 121.0, 120.0(4), 120.0(0), 92.5, 55.7(3), 55.6(6), 42.6(4), 42.6(2), 17.2, 14.4. λ_{max}(CH_2Cl_2)/nm: 337 (log ε/dm^3 mol^{-1} cm^{-1} 4.37), 308 sh (4.03) 252 (4.32), 243 (4.31). (MALDI-TOF, Dith) Anal. Calcd for $C_{38}H_{40}BrI$: 702.1 (94%), 703.1 (39%), 704.1 (100%), 705.1 (39%), 706.1 (8%). Found: 702.4 (89%), 703.4 (51%), 704.4 (100%), 705.4 (44%), 706.4 (10%); mp 276−277 °C.

7-{3,5-Bis[4-(2-ethylhexyloxy)phenyl]phenyl}-7′-bromo-9,9,9′,9′-tetra-n-propyl-2,2′-bifluorene (***2***). A mixture of **1** (250 mg, 0.355 mmol), 2-{3,5-bis[4-(2-ethylhexyloxy)phenyl]phenyl}-4,4,5,5-tetramethyl-1,3,2-dioxaborolane[41] (207 mg, 0.338 mmol), aqueous potassium carbonate (2 M, 2 mL), toluene (5 mL), and *tert*-butanol (2 mL) was deoxygenated by sparging with nitrogen gas for 15 min. Tetrakis(triphenylphosphine)-palladium(0) (41 mg, 0.036 mmol) was then added, and the mixture was deoxygenated for a further 10 min. The reaction was heated at 60 °C and stirred vigorously for 3 d. Upon cooling the mixture was diluted with toluene (10 mL) and water (10 mL), and the layers were separated. The aqueous phase was extracted with toluene (15 mL), and the combined organic phases were washed with brine (20 mL), dried over magnesium sulfate, and filtered. The filtrate was evaporated under reduced pressure to afford a crude brown solid, which was purified by column chromatography over silica using a dichloromethane:*n*-hexane mixture (15:85) as eluent to give **2** as a white solid (233 mg, 65%). Found: C 81.1, H 8.2 ($C_{72}H_{85}BrO_2$ requires C 81.4, H 8.1). ^{1}H NMR (500 MHz, $CHCl_3$) δ [ppm]: 7.48−7.85 (m, 19H, Fl-H, bp-H and sp-H), 7.05 (AA′BB′, 4H, sp-H), 3.90−4.00 (m, 4H, OCH_2), 1.95−2.15 (m, 8H, Pr−H), 1.75−1.84 (m, 2H, EtHeO CH), 1.30−1.62 (m, 16H, EtHeO CH_2), 0.90−1.05 (m, 12H, EtHeO CH_3), 0.70−0.90 (m, 20H, Pr−H). ^{13}C NMR (125 MHz, $CHCl_3$) δ [ppm]: 159.2, 153.2, 151.8, 151.7, 151.1, 142.6, 142.1, 141.0, 140.3(1), 140.3(0), 140.1(5), 141.0(9), 139.8, 139.2, 133.6, 130.0, 128.4, 126.3(0), 126.2(7), 126.2(2), 126.1(8), 124.4, 124.2, 121.8, 121.3(9), 121.3(6), 121.0, 120.9(7), 120.0(2), 120.0(1), 119.9(9), 114.9, 70.6, 55.7, 55.6, 42.8, 42.7, 39.4, 30.5, 29.1, 23.9, 23.1, 17.3, 17.2, 14.6, 14.5, 14.1, 11.1. λ_{max}(CH_2Cl_2)/nm: 345 (log ε/dm^3 mol^{-1} cm^{-1} 4.90), 281 (4.66), 310 sh (4.50), 256 (4.62). (MALDI-TOF, Dith) Anal. Calcd for $C_{72}H_{85}BrO_2$: 1060.6 (76%), 1061.6 (62%), 1062.6 (100%), 1063.6 (68%), 1064.6 (25%), 1065.6 (7%). Found: 1060.8 (54%), 1061.9 (59%), 1062.8 (100%), 1063.8 (59%), 1064.8 (28%), 1065.9 (9%). T_g (scan rate: 200 °C/min) = 68 °C.

7-{3,5-Bis[4-(2-ethylhexyloxy)phenyl]phenyl}-7′-(4,4,5,5,-tetramethyl-1,3,2-dioxaborolanyl)-9,9,9′,9′-tetra-n-propyl-2,2′-bifluorene (***3***). A vessel containing **2** (390 mg, 0.367 mmol) was deoxygenated by applying a vacuum and then backfilling with nitrogen. The solid was dissolved in tetrahydrofuran (2 mL) and cooled in a dry ice/acetone bath before adding *n*-butyllithium (1.6 M in hexanes, 0.28 mL, 0.44 mmol). The reaction was left to stir for 10 min. 2-Isopropoxy-4,4,5,5-tetramethyl-1,3,2-dioxaborolane (0.15 mL, 0.734 mmol) was added, and the reaction was stirred for 20 min before allowing it to warm to room temperature and stirring for a further 16 h. The mixture was finally heated to 55 °C and stirred for 2 h and then allowed to cool to room temperature. Dichloromethane (20 mL) was added, and the solution washed with water (2 × 20 mL) and brine (20 mL), dried over magnesium sulfate, and then filtered. The filtrate was evaporated to afford a crude yellow solid. The residue was purified by precipitation from dichloromethane (5 mL) into methanol (60 mL). The precipitate was recovered by centrifugation (3000 rpm, 5 min) and dried to give **3** as a white solid (335 mg, 82%). Found: C 84.3, H 8.9 ($C_{78}H_{97}BO_4$ requires C 84.4, H 8.8). ^{1}H NMR (500 MHz, $CHCl_3$) δ [ppm]: 7.81−7.87 (m, 5H, bp-H and/or Fl-H), 7.79 (d, 2H, J = 1.5 Hz, bp-H), 7.77 (dd, 1H, J = 7.5 and 0.5 Hz, Fl-H), 7.65−7.74 (m, 11H, bp-H and/or Fl-H and sp-H), 7.06 (AA′BB′, 4H, sp-H), 3.92−3.97 (m, 4H, OCH_2), 2.02−2.15 (m, 8H, Pr−H), 1.75−1.84 (m, 2H, EtHeO CH), 1.34−1.62 (m, 28H, EtHeO CH_2 and pin-CH_3), 0.92−1.00 (m, 12H, EtHeO CH_3), 0.70−0.89 (m, 20H, Pr−H). ^{13}C NMR (125 MHz, $CHCl_3$) δ [ppm]: 159.2, 152.1, 151.7(8), 151.7(6), 150.2, 143.8, 142.7, 142.1, 141.0, 140.5, 140.3, 140.2, 140.1, 140.0, 133.8, 133.6, 128.9, 128.4, 126.2(4), 126.2(0), 126.1, 124.4, 124.3, 121.8, 121.4, 120.3, 120.0, 119.0, 114.9, 83.7, 70.6, 55.6, 55.5, 42.8, 42.7, 39.4, 30.5, 29.1, 24.9, 23.9, 23.1, 17.3, 17.2, 14.6, 14.5, 14.1, 11.1. λ_{max}(CH_2Cl_2)/nm: 349 (log ε/dm^3 mol^{-1} cm^{-1} 4.91), 308 sh (4.45), 281 (4.63), 257 (4.62), 248 sh (4.60). (MALDI-TOF, DCTB) Anal. Calcd for $C_{78}H_{97}BO_4$: 1107.8 (20%), 1108.7 (100.0%), 1109.8 (79%), 1110.8 (34%), 1111.8 (9%). Found: 1108.2 (20%), 1109.2 (100%), 1110.2 (77%), 1111.2 (29%), 1112.2 (7%). T_g (scan rate: 200 °C/min) = 95 °C.

1,3,5,7-Tetrakis-[4-(7′-{3,5-bis[4-(2-ethylhexyloxy)phenyl]phenyl}-9,9,9′,9′-tetra-n-propyl-2,2′-bifluoren-7-yl)phenyl]adamantane (*D2*). A mixture of **3** (0.33 g, 0.30 mmol), 1,3,5,7-tetrakis(4-iodophenyl)adamantane[42] (**4**) (35 mg, 0.04 mmol), aqueous tetraethylammonium hydroxide (20 wt %, 1 mL), and toluene (3 mL) was deoxygenated by ultrasonication at reduced pressure for 3 min. The vessel was backfilled with argon before adding tetrakis-(triphenylphosphine)palladium(0) (17 mg, 0.02 mmol) and

deoxygenating a second time. The reaction was heated at 90 °C and stirred vigorously for 4 days. Upon cooling the mixture was diluted with toluene (10 mL) and hydrochloric acid (1 M, 10 mL). The layers were separated, and the aqueous phase was extracted with toluene (10 mL). The combined organic fractions were washed with brine (2 × 10 mL), dried over magnesium sulfate, and filtered. The solvent was removed to leave a brown solid. The residue was purified in three steps: first, column chromatography over silica using a dichloromethane:*n*-hexane mixture (40:60) as eluent; second, column chromatography over silica using a dichloromethane:*n*-hexane mixture (30:70) as eluent; and finally, the fractions containing a mixture of 2-, 3-, and 4-armed materials were separated by chromatotron chromatography (1 mm silica plate) eluting with dichloromethane:*n*-hexane mixture (15:85 → 26:74) to give D2 as a white solid (52 mg, 32%). Found: C 88.4, H 8.6 ($C_{322}H_{368}O_8$ requires C 88.6, H 8. 5). ^{1}H NMR (500 MHz, $CHCl_3$) δ [ppm]: 7.65−7.87 (brm, 92H, Fl-H, sp-H and bp-H), 7.06 (brAA′BB′, 16H, sp-H), 3.91−3.98 (brm, 16H, OCH_2), 2.41 (brs, 12H, Ad-H_2), 2.12 (brs, 32H, Pr−H), 1.75−1.85 (m, 8H, EtHeO CH), 1.33−1.62 (m, 64H, EtHeO CH_2), 0.92−1.02 (m, 48H, EtHeO CH_3), 0.66−0.92 (m, 80H, Pr−H). ^{13}C NMR (125 MHz, $CHCl_3$) δ [ppm]: 159.2, 151.8(1), 151.7(9), 151.7(6), 151.7(3), 148.4, 142.7, 142.1, 140.5(3), 140.4(9), 140.3, 140.2, 140.0(4), 139.9(7), 139.7, 133.6, 128.4, 127.2, 126.2, 125.6, 124.4, 124.3, 121.8, 121.6, 121.4, 120.0, 114.9, 70.6, 55.6, 55.5, 47.5(br), 42.9, 39.4, 39.3, 30.6, 29.1, 23.9, 23.1, 17.4, 14.5(8), 14.5(7), 14.1, 11.1. λ_{max}-(THF)/nm: 354 (log ε/dm^3 mol^{-1} cm^{-1} 5.62), 313 sh (5.10), 280 sh (5.26), 264 (5.37), 248 sh (5.25). (MALDI-TOF, DCTB) Anal. Calcd for $C_{322}H_{368}O_8$: *m*/*z*: 4362.8 (13%), 4363.8 (47%), 4364.8 (82%), 4365.9 (100.0%), 4366.8 (89%), 4367.8 (65%), 4368.9 (39%), 4369.8 (20%), 4370.8 (9%). Found: 4363.3 (12%), 4364.2 (45%), 4365.2 (78%), 4366.2 (100%), 4367.2 (83%), 4368.2 (61%), 4369.1 (35%), 4370.1 (17%), 4371.1 (7%). $T_{5\%}$ 420 °C; melting point >250 °C; $E_{1/2(Ox)}$ 0.85 V, $E_{1/2(Red)}$ −2.77 V relative to the ferrocenium/ferrocene couple.[36]

Results and Discussion

Synthesis. The synthesis of D1 has been reported previously.[22] D2 was prepared via the convergent route shown in Scheme 1. The advantage of using a convergent strategy over a divergent route[43] is that it avoids the difficult removal at each iterative step of the byproducts from incomplete reactions. Having the dendron and bifluorene chromophore as a complete unit before attachment to the adamantyl center reduces the number of multiple-site reactions to one. In the first step of the synthesis 7-bromo-9,9,9′,9′-tetra-*n*-propyl-2,2′-bifluorene[40] was iodinated at the 7′-position by reaction with *N*-iodosuccinimide and trifluoroacetic acid in chloroform at 60 °C, affording compound **1** in an 89% yield. Next, a palladium-catalyzed Suzuki coupling was performed to selectively replace the iodide with the first-generation biphenyl dendron that had 2-ethylhexyloxy surface groups.[41] By keeping the reaction at 60 °C and using just under 1 equiv of the 2-{3,5-bis[4-(2-ethylhexyloxy)phenyl]phenyl}-4,4,5,5-tetramethyl-1,3,2-dioxaborolane, only the iodine was replaced, and the monodendronized material **3** was isolated in a yield of 65%. To prepare the arm **3** for attachment to the adamantyl center **2** was treated with *n*-butyllithium at low temperature, followed by quenching the resultant aryl anion with 2-isopropoxy-4,4,5,5-tetramethyl-1,3,2-dioxaborolane. It was found that **3** could be simply purified by precipitation from a dichloromethane/methanol mixture to afford the desired product in an 82% yield. Finally, D2 was prepared in a 32% yield via Suzuki coupling of an excess of **3** with 1,3,5,7-tetrakis(4-iodophenyl)adamantane (**4**). The actual yield of D2 was higher, but the careful chromatography that was needed to remove it from compounds with fewer arms meant that there were additional losses. Given the similarity of the retention factors (R_f) of D2 and these impurities, we found that the best method for identifying the pure fractions from chromatography over silica was to use gel permeation chromatography[43] in combination with MALDI-TOF mass spectrometry.

Scheme 1. Synthesis of Dendrimer D2[a]

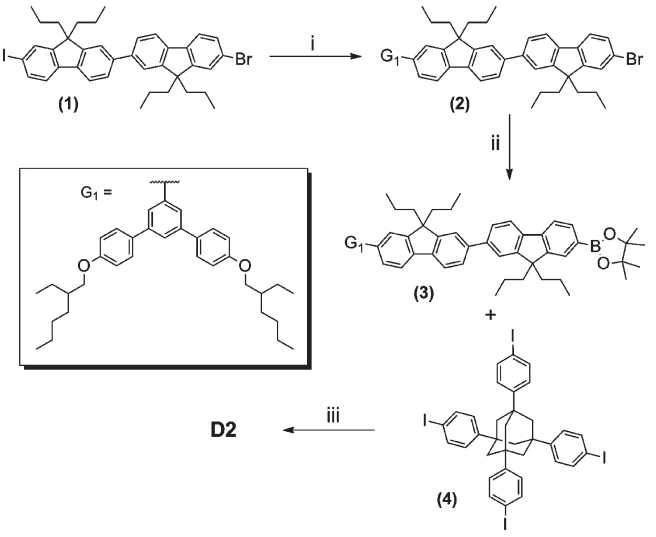

[a] Reagents and conditions: (i) G1-B(OCMe$_2$)$_2$, Pd(PPh$_3$)$_4$, K_2CO_3-(aq), toluene, *tert*-butanol, 60 °C, 3 days; (ii) *n*-butyllithium, tetrahydrofuran, −78 °C and then 2-isopropoxy-4,4,5,5-tetramethyl-1,3,2-dioxaborolane, RT, 16 h and then 55 °C for 2 h; (iii) Pd(PPh$_3$)$_4$, Et$_4$NOH(aq), toluene, 90 °C, 4 days.

(Photo)physical Properties. D1, D2, and PFO are all amorphous solids at room temperature and are readily soluble in common organic solvents such as dichloromethane, toluene, and tetrahydrofuran. Both D1 and D2 are thermally stable to high temperatures, showing a 5% loss of mass above 400 °C. Figure 2 shows the absorption and emission spectra of all three compounds in tetrahydrofuran solution. Table 1 summarizes the photophysical properties of the three compounds. The first thing to note is that the UV−vis and PL spectra of D1 and D2 are essentially identical. This shows that the 7,7′-diphenyl-9,9,9′,9′-tetra-*n*-propyl-2,2′-bifluorene chromophore is, as expected, effectively the same in each compound. Both the absorption and emission spectra for PFO are red-shifted by approximately 30 and 20 nm, respectively, when compared with the two dendrimers, and this is due to the effective chromophore having a longer conjugation length.[35,44] The photoluminescence quantum yield (PLQY) for all three compounds was close to 90% in tetrahydrofuran solution.

Fluorescence Quenching. The analytes used in this study were 1,4-dinitrobenzene (DNB), 2,4-dinitrotoluene (DNT), 4-nitrotoluene (pNT), 2,3-dimethyl-2,3-dinitrobutane (DMNB), benzophenone (BP), and duroquinone (DQ). Of these DNB, DNT, and pNT are nitroaromatic compounds, chosen because they are structurally similar to the well-known explosive 2,4,6-trinitrotoluene (TNT). In fact, DNB and DNT are decomposition products of TNT.[3,45] DNT is also recognized as an important analyte in its own right as it is present as an impurity in virtually all industrially manufactured TNT, and its higher vapor pressure means it is often easier to detect than TNT itself.[3] As mentioned previously, DMNB is a nitroaliphatic compound used as a taggant, which is added to plastic explosives during manufacture. BP and DQ are non-nitrated, high electron affinity aromatic compounds.

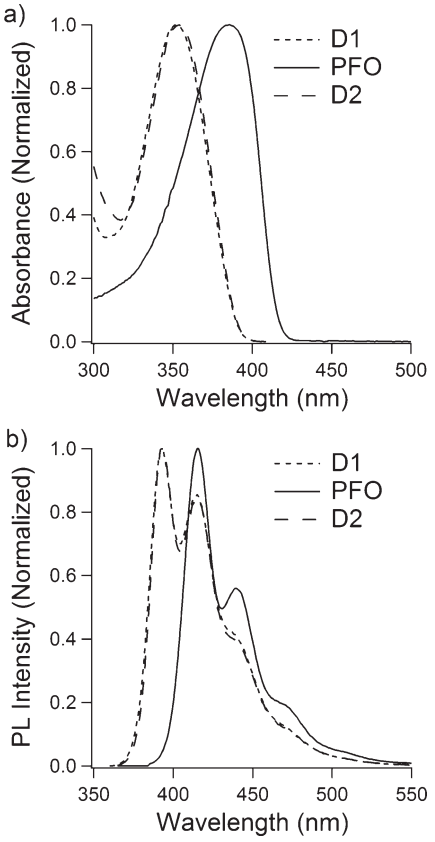

Figure 2. (a) Normalized absorbance spectra for the three compounds in tetrahydrofuran solution. (b) Normalized photoluminescence emission spectra for dilute solutions (absorbance ~0.1) of D1 (ex 352 nm), PFO (ex 385 nm), and D2 (ex 354 nm).

Table 1. Photophysical Properties of the Sensing Materials in Tetrahydrofuran Solution: (a) Relative to Quinine Sulfate; (b) Fluorescence Lifetime

	peak absorbance (nm)	peak emission (nm)	PLQY (%)[a]	τ (ps)[b]
D1	352	393	92	760
PFO	385	416	88	440
D2	354	393	88	670

These were chosen to act as control analytes to test for selectivity of the sensor materials for nitrated compounds.

In order to quantify the quenching efficiencies of the six analytes with each sensing material, Stern−Volmer measurements were performed. During a Stern−Volmer analysis the photoluminescence intensity of the sensing material is measured while varying the concentration of the analyte (or quencher). It can be shown for a simple system that

$$\frac{F_0}{F} = 1 + K_{SV}[Q] \quad (3)$$

where F_0 is the photoluminescence intensity in the absence of a quencher, F is the photoluminescence intensity with quencher concentration [Q], and K_{SV} is the Stern−Volmer constant.[39] If quenching is caused by a single mechanism, a plot of F_0/F vs [Q] will provide a straight line with gradient K_{SV}. As most of the analytes used in this study strongly absorb UV light, a significant portion of the excitation is directly attenuated by the analyte, and it is important to analyze these Stern−Volmer data carefully. In addition, due to overlap of the analyte and sensor absorption spectra with the sensor emission spectra, a portion of the fluorescence will also be reabsorbed by the solution. Corrections to account

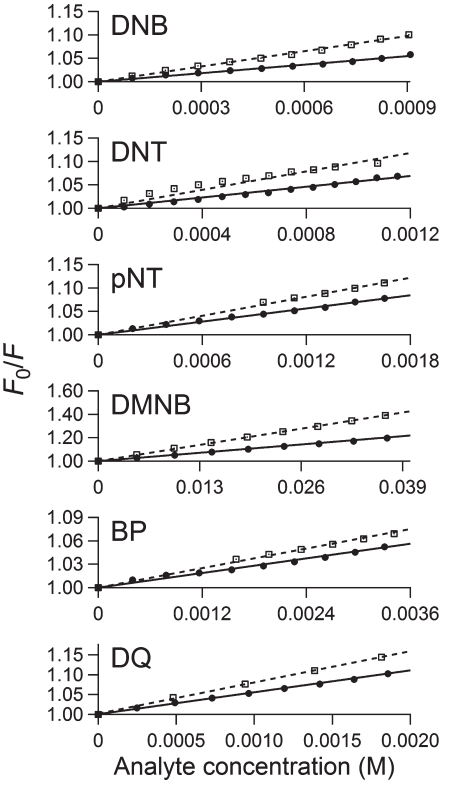

Figure 3. Steady-state Stern−Volmer plots and fits (using eq 3) for D1 (solid circles and solid lines) and D2 (open squares and dashed lines) with the six analytes.

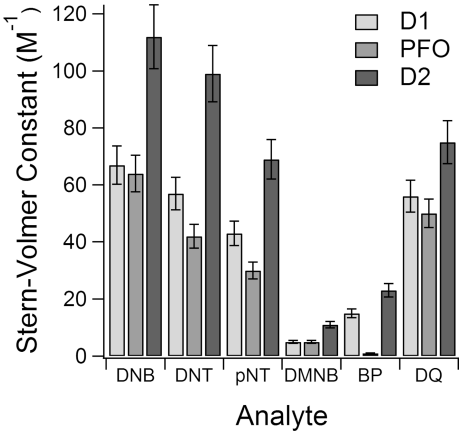

Figure 4. Steady-state Stern−Volmer constants for all three sensing materials with each analyte. Constants are averages of between 2 and 4 runs. Error bars represent 10% uncertainty.

for these two effects have been described previously[21,38] and have been applied to these results.

Figure 3 shows representative Stern−Volmer plots for D1 and D2 with all six of the analytes. The data appears linear, which in many studies has been ascribed there being only a single quenching mechanism, but as will be discussed later this is not necessarily the case. The data was fitted with eq 3, and the resulting Stern−Volmer constants (K_{SV}) for the three sensing materials for each of the analytes are shown in Figure 4. Quenching was observed with all sensor−analyte combinations, except for PFO with BP, which showed no significant quenching. The K_{SV}s are comparable to reported values for other fluorescent sensors in solution.[9,13,15,46,47] However, a key result from the measurements is that the

"three-dimensional" D2 has larger K_{SV}s than the planar D1 and PFO. In addition, both dendrimers exhibit consistently higher K_{SV}s than PFO, indicating greater sensitivities toward the analytes.

For all three sensing materials, the quenching constants for nitroaromatics can be ordered DNB > DNT > pNT. Remembering that oxidative fluorescence quenching requires the analyte molecule to accept an excited electron from the sensing material, it is interesting to note the reduction potentials for these three analytes are −0.7, −1.0, and −1.2 V, respectively [relative to the standard calomel electrode (SCE)].[20] This trend reinforces the idea that one of the major factors that determine quenching efficiencies in solution is the electron affinity of the analyte. That is, the highest electron affinity analyte, DNB, is the most efficient quencher, and the lowest electron affinity nitroaromatic analyte, pNT, is the least efficient quencher. DQ has a reduction potential of −0.8 V,[20] and consequently for D1 and PFO the quenching efficiency sits between that of DNB and DNT as might be predicted. However, for D2, the quenching efficiency of DQ is approximately the same as pNT and is significantly less than that for DNT. This suggests the quenching interaction of DQ with D2 is less favorable relative to the nitroaromatic compounds than with D1 or PFO. BP has a reduction potential of −1.6 V[20] and shows much lower quenching efficiencies with both D1 and D2 than the other aromatic analytes. DMNB has a reduction potential of −1.7 V (vs SCE)[48] and on average shows the lowest quenching constants of the nitrated analytes tested.

While the steady-state Stern−Volmer measurements provide some insight into the overall quenching efficiency of each analyte, one shortcoming of this type of analysis is that the mechanism of quenching cannot easily be determined. Quenching that is caused by formation of a nonemissive ground-state complex between the sensing compound and an analyte (so-called static quenching) is indistinguishable from quenching caused by a fleeting collision of the excited-state sensing compound with an analyte (collisional quenching). It is clear that collisional quenching will result in a change in fluorescence lifetime as the analyte concentration varies, whereas this will not occur with static quenching. As a consequence, the role of collisional quenching in analyte detection can be probed by time-resolved PL. For a collisional quenching mechanism it can be shown that

$$\frac{\tau_0}{\tau} = 1 + K_C[Q] \tag{4}$$

where τ_0 is the fluorescence lifetime of the sensor material in the absence of a quencher, τ is the fluorescence lifetime of the sensing compound with quencher concentration [Q], and K_C is the collisional Stern−Volmer constant.[39] If the quenching of the PL is entirely collisional, that is, there is no static quenching, then K_C will be equal to K_{SV}. If the quenching mechanism is entirely static, changes in analyte concentration will have no effect on the fluorescence lifetime of the sensing material and K_C will be 0. If a combination of both static and collisional quenching mechanisms is occurring, then it can be shown for the steady state measurement that

$$\frac{F_0}{F} = (1 + K_C[Q])(1 + K_S[Q])$$
$$= 1 + (K_C + K_S)[Q] + K_C K_S[Q]^2 \tag{5}$$

where K_S is the static Stern−Volmer constant, representing quenching by a dark ground-state complex between the sensing material and the analyte.[39] The resulting plot of F_0/F vs [Q] should be quadratic as opposed to linear, as would be expected from eq 3. At first glance it would seem unlikely that the data in Figure 3 could be caused by a combination of mechanisms because it is linear with analyte concentration. However, when [Q] is very low, the term $[Q]^2$ in eq 5 becomes vanishingly small, and the plot would appear to be linear with a gradient equal to $K_C + K_S$.[23] As stated previously, due to the strong absorbance of the analytes at the excitation wavelengths used in this study, it was necessary to keep the concentration of the analytes very low in order to limit the maximum total absorbance to ~0.6. Therefore, these results are in the linear regime of eq 5.

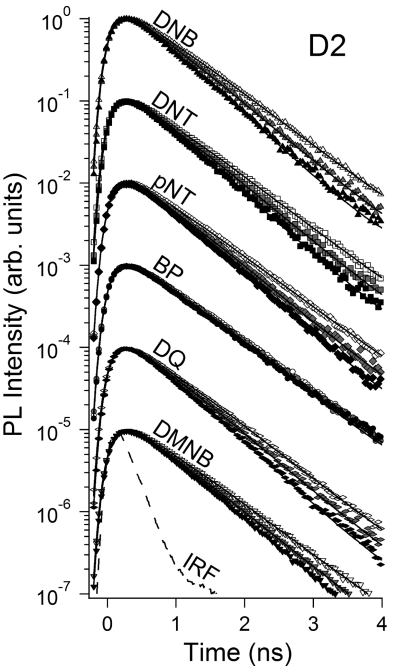

Figure 5. Fluorescence decays (symbols) and fits (lines) for D2 with three concentrations of each analyte. DNB, DNT, pNT, DQ: 0 M (unfilled), 0.004 M (gray), 0.008 M (black); BP, DMNB: 0 M (unfilled), 0.010 M (gray), 0.019 M (black). Each analyte is offset for clarity. The instrument response function (IRF) is shown by a dashed line.

Time-correlated single photon counting (TCSPC) spectroscopy was used to measure the fluorescence lifetimes of the three sensing materials in the absence and presence of different analyte concentrations in order to determine whether collisional quenching, static quenching, or a combination of the two mechanisms was occurring. In the absence of the analytes all three sensing compounds had fluorescence decays that could be represented with a single-exponential fit (Figure 5; D2 is shown as being representative of all three sensing compounds). Apart from PFO with BP, all three sensing molecules also showed a decrease in fluorescence lifetime as analyte concentrations were increased, indicating that a collisional quenching mechanism was at least in part occurring. The fluorescence lifetimes in the presence of the analytes (Figure 5) could also be fitted with a single-exponential decay, and hence K_C could be calculated. Importantly, the values of K_C obtained from these measurements were, in every case, lower than the respective values of K_{SV}, and hence it can be concluded that a combination of static and collisional quenching is occurring with these sensing materials. The results also confirm that it is the low analyte concentration ranges used which gives rise to apparent linearity of the steady-state Stern−Volmer plots. This result is in contrast to reported polymer sensors, which exhibit

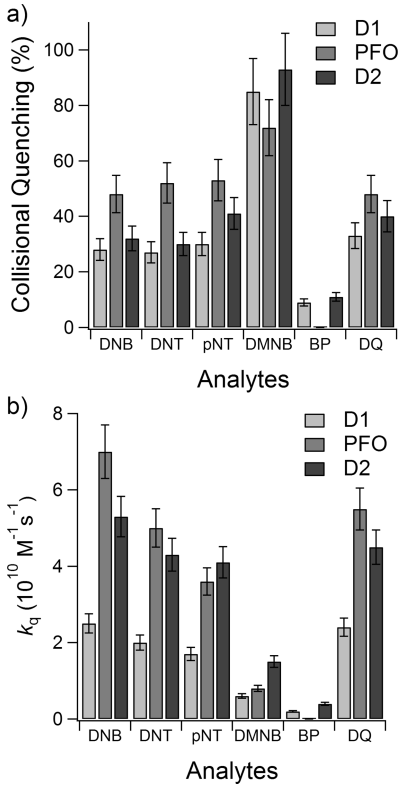

Figure 6. (a) Percentage of overall quenching that is due to a collisional mechanism. (b) Bimolecular collisional quenching rates (k_q).

purely static quenching.[47,49] We have previously reported two dendrimers with triphenylamine centers, thiophene units and the same dendrons as D1 and D2, which show almost purely collisional quenching.[23] It is therefore clear that dendrimers with different quenching mechanisms can be engineered at the molecular level if one understands the appropriate structure−property relationships.

As K_C and K_{SV} can be determined experimentally, it is possible to calculate K_S using eq 5. The fraction of collisional quenching can then be calculated and is shown as a percentage in Figure 6a. The first thing to note from Figure 6a is that both D1 and D2 have essentially the same ratio of collisional and static quenching for each of the analytes. For these two dendrimers, 30−40% of the quenching is collisional for all analytes with a single aromatic ring, only around 10% is collisional for BP, which contains two aromatic rings, and finally quenching by the nonaromatic analyte DMNB primarily occurs via a collisional mechanism. There is a strong correlation between the number of aryl rings present in the analyte and the collisional quenching percentage, with more aryl rings corresponding to more static quenching. This can be understood as both D1 and D2 contain large flat π-electron systems that can undergo π-stacking with the analytes, which is reported to be the main reason for strong static quenching in some polymeric sensing materials.[47,49] The link between the number of aryl rings in the analyte and the ratio of quenching mechanisms is also apparent for PFO; however, PFO shows ~50% collisional quenching for the single ring analytes and around 70% collisional for DMNB. It is noted again that PFO is unquenched by BP. The difference in ratio between collisional and static quenching for PFO and the dendrimers may be due to a difference in the nature of the emissive chromophore in conjugated polymers and the dendrimers. In the dendrimers the emissive chromophores are well-defined with breaks in the π-electron delocalization caused by the connectivity (regiochemistry) of the individual groups. Often there will be a single emissive chromophore in a dendrimer. Conjugated polymers, on the other hand, can be thought of as being comprised of a number of "chromophores" or fluorescent segments separated by conformational effects such as twists. For a polymer it is possible for an analyte to bind to one or more "chromophores" along the polymer chain with another segment being photoexcited. The exciton can then migrate intramolecularly to the quenching site (the "chromophore" to which the analyte is bound). This is still static quenching as the analyte is bound to the polymer chain but differs from classic static quenching in that the polymer is still able to be photoexcited rather than there being a dark state. This process has been previously described as amplification of sensing by polymers. Because of exciton migration, excitons formed on chains with bound analytes will have shorter lifetimes, an effect normally associated with collisional quenching. Therefore, for PFO the TRPL measurements give an over estimation of the collisional component.

Using the time-resolved data, the bimolecular collisional quenching rate for each sensing material and analyte combination can be calculated[39] as

$$k_q = \frac{K_C}{\tau} \tag{6}$$

with the results shown in Figure 6b. For DNB, DNT, pNT, and DQ the collisional quenching rates are in the range $(1.7-7) \times 10^{10}$ M^{-1} s^{-1}. That is, the collisional quenching is essentially diffusion controlled and highly efficient. The rates for DMNB and BP are slightly lower, but still in the 10^9-10^{10} M^{-1} s^{-1} range. It is likely that collisional quenching by these latter two analytes is still diffusion controlled; however, fewer collisions result in quenching. For electron transfer and hence quenching to occur, it is necessary for the analyte to have a suitable electron affinity and for the analyte and sensor to be in the correct molecular orientation for electron transfer to occur. Both DMNB and BP have electron affinities close to the limit required for detection, and hence the fact that some collisions do not result in luminescence quenching could plausibly arise from the incorrect orientation of the analyte and sensor to allow for electron transfer. That is, the rate of electron transfer from the excited sensor to the analyte is both energy and orientation dependent. It is interesting to note that D1 has significantly lower bimolecular collisional quenching rates than either PFO or D2. It is thought that this difference arises from the smaller size of D1 compared to PFO and D2, resulting in a reduced collisional radius. Also, PFO has a slightly higher calculated bimolecular quenching rate than D2 for DNB, DNT, and DQ. This may simply be caused by the larger collisional radius of the long polymer chains or possibly by convolution of the collisional quenching with the delayed static quenching.

Finally, the overall greater quenching efficiency of the analytes with D2 compared to D1 and PFO can be ascribed to an amplification effect of the four chromophores in close proximity. It has been shown that rapid exciton migration occurs between chromophores on the surface of flexible dendritic scaffolds.[26] D1 contains a single emissive bifluorene containing chromophore per dendrimer, and hence interaction of one dendrimer with one analyte can only quench one exciton. PFO and D2 both contain a number of chromophores with D2 containing four independently emissive units held in a tetrahedral arrangement. This means that an exciton formed on one chromophore could hop

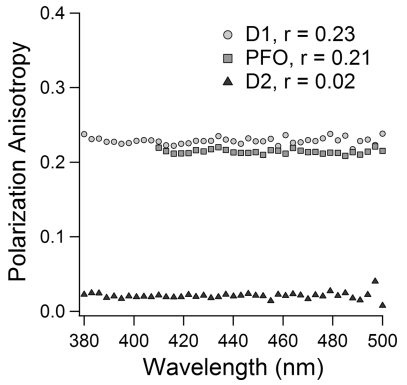

Figure 7. Steady-state fluorescence polarization anisotropy for all three sensing materials in tetrahydrofuran solution. Average polarization anisotropy ratios in the displayed wavelength range are shown in the legend.

rapidly between the other arms before decaying with emission of a photon. It is noted that there is a significant amount of overlap between the absorption and emission spectra for D2, suggesting resonant energy transfer (RET) between appropriately oriented chromophores should be efficient. In order to test this hypothesis, steady-state fluorescence polarization anisotropy measurements were performed with all three sensing materials with the results shown in Figure 7. The average polarization anisotropy ratios for D1 and PFO are 0.23 and 0.21, respectively. These values are slightly lower than the idealized value of 0.4 for perfectly polarized emission in a solution, which is almost certainly caused by molecular rotations occurring on a similar time scale to the fluorescence lifetimes. The value of 0.21 for PFO also suggests that exciton migration between chromophores within each chain is inefficient, consistent with an extended chain conformation.[50] Because of its larger size, the rotational correlation time for D2 should be longer than for D1 in the same solvent, which would predict a larger anisotropy ratio for D2 than D1. However, the average anisotropy ratio for D2 is almost 0; that is, the emission is fully depolarized. This is strong evidence to suggest that excitons in D2 rapidly move between the four chromophores on a time scale much shorter than the emissive lifetime. This very fast process in D2 is beyond the resolution of the TCSPC instrumentation used in our lifetime measurements, and therefore any delayed static quenching would not inflate the calculated bimolecular collisional quenching rate. We propose that a quenching interaction of one analyte molecule with a chromophore of one arm of D2 would cause excitons formed on any of the four arms to be quenched, leading to an amplification in signal akin to those reported for polymer sensors.[18]

Conclusions

We have synthesized and studied in detail two highly fluorescent dendrimers based upon near identical fluorene-based chromophores but with very different degrees of dimensionality. We have compared the explosive analyte sensing ability and photophysics of these dendrimers to the related polymer PFO and built consistent structure−property relationships to explain the underlying mechanisms. The more 3-dimensional dendrimer D2 is quenched more efficiently by a range of nitroaromatic analytes than D1 or PFO. The ratio of quenching mechanisms is the same in both the dendrimers: 30−40% collisional for analytes with one aryl ring, only 10−20% collisional for analytes with two aryl rings, and primarily collisional for aliphatic analytes. We postulate that the increased quenching efficiency arises from an amplification effect in D2, which has multiple identical chromophores that can all be quenched by a single analyte interaction. Finally, D2 is quenched less by the control analyte DQ relative to the nitroaromatic analytes when compared with D1 and PFO. These results suggest that the physical shape of the sensing compound plays a very important role in sensitivity and selectivity of fluorescent sensors for explosives.

Acknowledgment. Prof. Paul Burn is the recipient of an Australian Research Council Federation Fellowship (Project FF0668728) and Prof. Paul Meredith is a Queensland Smart State Senior Fellow. Mr. Hamish Cavaye is supported by an Endeavour International Postgraduate Research Scholarship and University of Queensland Living Allowance Scholarship. The research was supported by the Australian Research Council through the Discovery Program (DP0986838). The Centre for Organic Photonics & Electronics is a strategic initiative of the University of Queensland. The authors express thanks and acknowledge the assistance of Dr. Mark Fernee with the TRPL experiments.

References and Notes

(1) Trogler, W. C. In *NATO ASI Workshop, Electronic Noses & Sensors for the Detection of Explosives*; Kluwer Academic Publishers: Dordrecht, The Netherlands, 2004.
(2) Czarnik, A. W. *Nature* **1998**, *394*, 417–418.
(3) George, V.; Jenkins, T. F.; Leggett, D. C.; Cragin, J. H.; Phelan, J.; Oxley, J.; Pennington, J. *Proc. SPIE* **1999**, *3710*, 258–269.
(4) Moore, D. S. *Rev. Sci. Instrum.* **2004**, *75* (8), 2499–2512.
(5) Spangler, G. E.; Carrico, J. P.; Campbell, D. N. *J. Test. Eval.* **1985**, *13* (3), 234–240.
(6) Dorozhkin, L. M.; Nefedov, V. A.; Sabelnikov, A. G.; Sevastjanov, V. G. *Sens. Actuators, B* **2004**, *99* (2−3), 568–570.
(7) Forzani, E. S.; Lu, D. L.; Leright, M. J.; Aguilar, A. D.; Tsow, F.; Iglesias, R. A.; Zhang, Q.; Lu, J.; Li, J. H.; Tao, N. J. *J. Am. Chem. Soc.* **2009**, *131* (4), 1390–1391.
(8) McGill, R. A.; Mlsna, T. E.; Chung, R.; Nguyen, V. K.; Stepnowski, J. *Sens. Actuators, B* **2000**, *65* (1−3), 5–9.
(9) Meaney, M. S.; McGuffin, V. L. *Anal. Chim. Acta* **2008**, *610* (1), 57–67.
(10) Meaney, M. S.; McGuffin, V. L. *Anal. Bioanal. Chem.* **2008**, *391* (7), 2557–2576.
(11) Andrew, T. L.; Swager, T. M. *J. Am. Chem. Soc.* **2007**, *129* (23), 7254–7255.
(12) Germain, M. E.; Knapp, M. J. *Chem. Soc. Rev.* **2009**, *38* (9), 2543–2555.
(13) Germain, M. E.; Vargo, T. R.; Khalifah, P. G.; Knapp, M. J. *Inorg. Chem.* **2007**, *46* (11), 4422–4429.
(14) Lan, A. J.; Li, K. H.; Wu, H. H.; Olson, D. H.; Emge, T. J.; Ki, W.; Hong, M. C.; Li, J. *Angew. Chem., Int. Ed.* **2009**, *48* (13), 2334–2338.
(15) Kose, M. E.; Harruff, B. A.; Lin, Y.; Veca, L. M.; Lu, F. S.; Sun, Y. P. *J. Phys. Chem. B* **2006**, *110* (29), 14032–14034.
(16) Snow, E. S.; Perkins, F. K.; Houser, E. J.; Badescu, S. C.; Reinecke, T. L. *Science* **2005**, *307*, 1942–1945.
(17) McQuade, D. T.; Pullen, A. E.; Swager, T. M. *Chem. Rev.* **2000**, *100* (7), 2537–2574.
(18) Thomas, S. W.; Joly, G. D.; Swager, T. M. *Chem. Rev.* **2007**, *107* (4), 1339–1386.
(19) Toal, S. J.; Trogler, W. C. *J. Mater. Chem.* **2006**, *16* (28), 2871–2883.
(20) Yang, J. S.; Swager, T. M. *J. Am. Chem. Soc.* **1998**, *120* (46), 11864–11873.
(21) Cavaye, H.; Barcena, H.; Shaw, P. E.; Burn, P. L.; Lo, S.-C.; Meredith, P. *Proc. SPIE* **2009**, *7418*, 741803.
(22) Cavaye, H.; Smith, A. R. G.; James, M.; Nelson, A.; Burn, P. L.; Gentle, I. R.; Lo, S.-C.; Meredith, P. *Langmuir* **2009**, *25* (21), 12800–12805.
(23) Olley, D. A.; Wren, E. J.; Vamvounis, G.; Fernee, M. J.; Wang, X.; Burn, P. L.; Meredith, P.; Shaw, P. E. *Chem. Mater.*, DOI: 10.1021/cm1020355.
(24) Richardson, S.; Barcena, H. S.; Turnbull, G. A.; Burn, P. L.; Samuel, I. D. W. *Appl. Phys. Lett.* **2009**, *95*, 063305.
(25) Narayanan, A.; Varnavski, O. P.; Swager, T. M.; Goodson, T., III. *J. Phys. Chem. C* **2008**, *112* (4), 881–884.

(26) Guo, M.; Varnavski, O.; Narayanan, A.; Mongin, O.; Majoral, J. P.; Blanchard-Desce, M.; Goodson, T., III. *J. Phys. Chem. A* **2009**, *113* (16), 4763–4771.
(27) Germain, M. E.; Vargo, T. R.; McClure, B. A.; Rack, J. J.; Van Patten, P. G.; Odoi, M.; Knapp, M. J. *Inorg. Chem.* **2008**, *47* (14), 6203–6211.
(28) Yang, J. S.; Swager, T. M. *J. Am. Chem. Soc.* **1998**, *120* (21), 5321–5322.
(29) Fisher, M.; laGrone, M.; Sikes, J. *Proc. SPIE* **2003**, *5089*, 991–1000.
(30) Fisher, M.; Sikes, J.; Prather, M. *Proc. SPIE* **2004**, *5403*, 409–417.
(31) Hwang, S.-H.; Moorefield, C. N.; Newkome, G. R. *Chem. Soc. Rev.* **2008**, *37* (11), 2543–2557.
(32) Burn, P. L.; Lo, S.-C.; Samuel, I. D. W. *Adv. Mater.* **2007**, *19* (13), 1675–1688.
(33) Lo, S.-C.; Burn, P. L. *Chem. Rev.* **2007**, *107* (4), 1097–1116.
(34) Wang, P.-W.; Liu, Y.-J.; Devadoss, C.; Bharathi, P.; Moore, J. S. *Adv. Mater.* **1996**, *8* (3), 237–241.
(35) Klaerner, G.; Miller, R. D. *Macromolecules* **1998**, *31* (6), 2007–2009.
(36) Gagne, R. R.; Koval, C. A.; Lisensky, G. C. *Inorg. Chem.* **1980**, *19* (9), 2854–2855.
(37) Demas, J. N.; Crosby, G. A. *J. Phys. Chem.* **1971**, *75* (8), 991–1024.
(38) Zheng, M.; Bai, F. L.; Li, F. Y.; Li, Y. L.; Zhu, D. B. *J. Appl. Polym. Sci.* **1998**, *70* (3), 599–603.
(39) Lakowicz, J. R. In *Principles of Fluorescence Spectroscopy*, 2nd ed.; Kluwer Academic: Dordrecht, The Netherlands, 1999.
(40) Katsis, D.; Geng, Y. H.; Ou, J. J.; Culligan, S. W.; Trajkovska, A.; Chen, S. H.; Rothberg, L. J. *Chem. Mater.* **2002**, *14* (3), 1332–1339.
(41) Lo, S.-C.; Namdas, E. B.; Burn, P. L.; Samuel, I. D. W. *Macromolecules* **2003**, *36* (26), 9721–9730.
(42) Mathias, L. J.; Reichert, V. R.; Muir, A. V. G. *Chem. Mater.* **1993**, *5* (1), 4–5.
(43) Jeeva, S.; Moratti, S. C. *Synthesis* **2007**, *21*, 3323–3328.
(44) Schumacher, S.; Ruseckas, A.; Montgomery, N. A.; Skabara, P. J.; Kanibolotsky, A. L.; Paterson, M. J.; Galbraith, I.; Turnbull, G. A.; Samuel, I. D. W. *J. Chem. Phys.* **2009**, *131* (15), 154906.
(45) Jenkins, T. F.; Leggett, D. C.; Miyares, P. H.; Walsh, M. E.; Ranney, T. A.; Cragin, J. H.; George, V. *Talanta* **2001**, *54* (3), 501–513.
(46) Kim, Y.; Zhu, Z.; Swager, T. M. *J. Am. Chem. Soc.* **2004**, *126* (2), 452–453.
(47) Zhao, D.; Swager, T. M. *Macromolecules* **2005**, *38* (22), 9377–9384.
(48) Thomas, S. W., III.; Amara, J. P.; Bjork, R. E.; Swager, T. M. *Chem. Commun.* (*Cambridge, U. K.*) **2005**, 4572–4574.
(49) Sohn, H.; Sailor, M. J.; Magde, D.; Trogler, W. C. *J. Am. Chem. Soc.* **2003**, *125* (13), 3821–3830.
(50) Beljonne, D.; Pourtois, G.; Silva, C.; Hennebicq, E.; Herz, L. M.; Friend, R. H.; Scholes, G. D.; Setayesh, S.; Mullen, K.; Brédas, J. L. *Proc. Natl. Acad. Sci. U. S. A.* **2002**, *99* (17), 10982–10987.